

RESEARCH REPORT

Vegfa regulates perichondrial vascularity and osteoblast differentiation in bone development

Xuchen Duan, Yurie Murata, Yanqiu Liu, Claudia Nicolae, Bjorn R. Olsen and Agnes D. Berendsen*

ABSTRACT

Vascular endothelial growth factor A (Vegfa) has important roles in endochondral bone formation. Osteoblast precursors, endothelial cells and osteoclasts migrate from perichondrium into primary ossification centers of cartilage templates of future bones in response to Vegfa secreted by (pre)hypertrophic chondrocytes. Perichondrial osteolineage cells also produce Vegfa, but its function is not well understood. By deleting *Vegfa* in osteolineage cells *in vivo*, we demonstrate that progenitor-derived Vegfa is required for blood vessel recruitment in perichondrium and the differentiation of osteoblast precursors in mice. Conditional deletion of Vegfa receptors indicates that Vegfa-dependent effects on osteoblast differentiation are mediated by Vegf receptor 2 (Vegfr2). In addition, Vegfa/Vegfr2 signaling stimulates the expression and activity of Indian hedgehog, increases the expression of β -catenin and inhibits Notch2. Our findings identify Vegfa as a regulator of perichondrial vascularity and osteoblast differentiation at early stages of bone development.

KEY WORDS: Vascular endothelial growth factor A, Osteoblast differentiation, Bone development, Osteoblast precursor, Osterix, Indian hedgehog, β -catenin, Notch, Mouse

INTRODUCTION

During endochondral bone formation osteochondroprogenitors form cartilage templates of future bones. Following chondrocyte hypertrophy, perichondrial osteoblast precursors, endothelial and hematopoietic cells and osteoclasts migrate into primary ossification centers (POCs) and replace cartilage by bone marrow and trabecular bone (Karsenty, 2003; Kronenberg, 2003; Zelzer and Olsen, 2003).

The transcription factor osterix (Osx; Sp7 – Mouse Genome Informatics) is expressed in perichondrial osteoblast precursors and, at lower levels, in prehypertrophic chondrocytes (Nakashima et al., 2002). Osx expression first appears in the perichondrium of bone templates at embryonic day (E) 13.5 in mice. After E15.5, strong expression is associated with trabecular and cortical bone formation (Nakashima et al., 2002) as the precursors differentiate into collagen I (Col1)-expressing osteoblasts (Karsenty and Wagner, 2002; Maes et al., 2010b).

Several factors regulate endochondral bone formation, including Indian hedgehog (Ihh), Wnt/ β -catenin, Notch, Bmps, Fgfs and Pthrp (Kronenberg, 2003). Ihh induces osteoblast differentiation during perichondrial maturation into periosteum (Chung et al., 2001; Hu et al., 2005; Long et al., 2004). Canonical Wnt/ β -catenin signaling is essential for the differentiation of osteochondroprogenitors (Day

et al., 2005; Hill et al., 2005) and promotes hypertrophic chondrocyte differentiation and osteoblast differentiation and maturation (Hu et al., 2005). Notch2 is a negative regulator of osteoblast differentiation (Hilton et al., 2008).

Vegfa is essential during key stages of endochondral bone formation. Mice with *Vegfa* conditionally deleted in collagen II (Col2)-expressing cells show a delay in blood vessel invasion into POCs, delayed hypertrophic cartilage removal and chondrocyte apoptosis (Haigh et al., 2000; Zelzer et al., 2002, 2004). Mice expressing only the non-heparin-binding Vegf120 isoform of Vegfa show decreased skeletal mineralization and reduced expression of osteoblastic markers (Maes et al., 2002; Zelzer et al., 2002). Overexpression of Vegfa in osteochondroprogenitor cells results in increased bone mass (Maes et al., 2010a).

Osx-positive osteoblast precursors not only migrate into POCs in response to Vegfa secreted by chondrocytes, but they also express high levels of Vegfa (Maes et al., 2010b). In this study, we show that Vegfa produced by these cells is required for blood vessel recruitment and early stages of osteoblast differentiation in perichondrial regions of bone templates. This function is mediated by Vegfr2 and is likely to involve Ihh, β -catenin and Notch2-dependent pathways.

RESULTS AND DISCUSSION

Vegfa regulates bone formation during endochondral ossification

To assess the function of Vegfa expressed by Osx-positive precursor cells in developing bone, we generated mice with conditional loss of *Vegfa* alleles in these cells. Newborn *Vegfa^{fl/fl}; Osx-Cre:GFP* mice had thinner bones and reduced skeletal mineralization compared with wild-type (WT) (*Vegfa^{+/+}; Osx-Cre:GFP*) mice (Fig. 1A,B). MicroCT showed reduced tibia length and that secondary ossification centers were largely missing in mutants at postnatal day (P) 9 (supplementary material Fig. S1A). Mutant femurs had increased hypertrophic zones, decreased mineralization and fewer tartrate-resistant acid phosphatase (Trap)-positive osteoclasts and GFP-labeled Osx-expressing (*Osx/GFP⁺*) cells (Fig. 1B). Anti-CD31 (Pecam1) staining indicated reduced density of endothelial and *Osx/GFP⁺* cells within primary spongiosa in mutants (Fig. 1B).

Visualization of *Vegfa* expression by X-gal staining of P1 femurs from heterozygous *Vegfa-lacZ^{KI/WT}* (*Vegfa-lacZ*) mice revealed positive staining of prehypertrophic chondrocytes and cells located within primary spongiosa; by contrast, WT tissue showed only low-level false-positive staining in osteoclasts (supplementary material Fig. S1B). *In situ* hybridization indicated that loss of Vegfa expression in Osx⁺ precursors resulted in reduced *Col1* (*Colla1*)-expressing cells within primary spongiosa (Fig. 1C). Low *Col1* expression in mutant bones confirmed that the majority of *Osx/GFP⁺* cells are osteoblast progenitor cells, which are decreased in mutants (Fig. 1B,C).

Department of Developmental Biology, Harvard School of Dental Medicine, Boston, MA 02115, USA.

*Author for correspondence (Agnes_Berendsen@hsdm.harvard.edu)

Received 17 September 2014; Accepted 19 April 2015

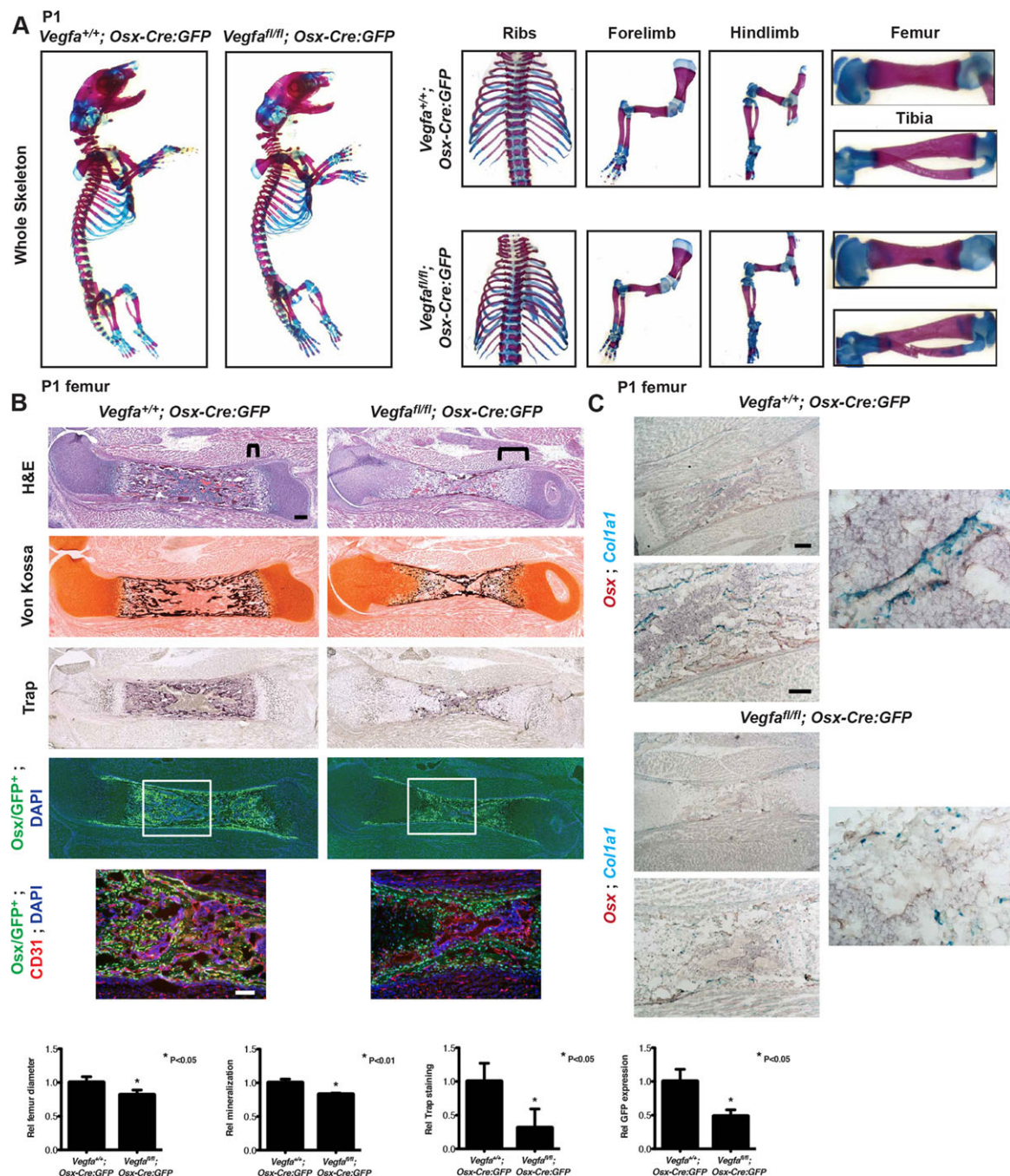


Fig. 1. Progenitor-derived Vegfa regulates mineralization in developing bones. (A) Whole-mount Alcian Blue and Alizarin Red stained skeletal preparations of P1 *Vegfa^{+/+}; Osx-Cre:GFP* and *Vegfa^{-/-}; Osx-Cre:GFP* mice. (B) Histology of P1 femurs of *Vegfa^{+/+}; Osx-Cre:GFP* and *Vegfa^{-/-}; Osx-Cre:GFP* mice by H&E (scale bar: 200 µm), von Kossa and Trap staining, *Osx/GFP⁺* expression and anti-CD31 staining (scale bar: 100 µm). The bracket indicates increased thickness of the growth plate region in mutant compared with control femur. The boxes indicate central regions of the primary ossification center (POC), similar to those shown at higher magnification beneath. Bar charts show quantification of bone diameter, mineralization, Trap staining and *Osx/GFP* expression in femur sections of P1 *Vegfa^{+/+}; Osx-Cre:GFP* ($n=3$) and *Vegfa^{-/-}; Osx-Cre:GFP* ($n=3$) mice. Mean±s.d. *P<0.05 or *P<0.01 for comparison between genotypes. (C) *In situ* hybridization on femur sections of P1 *Vegfa^{+/+}; Osx-Cre:GFP* and *Vegfa^{-/-}; Osx-Cre:GFP* mice for *Osx* (red) and *Col1a1* (turquoise) (scale bars: 200 µm, top; 100 µm, bottom). To the right are magnified views of *Osx* and *Col1a1* expression in femoral POC.

Vegfa stimulates perichondrial vascularity and osteoblast differentiation

To address mechanisms underlying reduced numbers of *Osx*⁺ cells in P1 femurs, we analyzed *Osx/GFP⁺* cells during formation of POCs. E15.5 tibia of mutant mice showed markedly decreased numbers of *Osx/GFP⁺* cells (43.2±4.9 per defined region of perichondrium and POC) compared with WT (56.4±6.5) mice

(Fig. 2A). The area of anti-CD31 staining in POCs as a percentage of stained areas in perichondrium and POC combined was 0.6±0.5% for mutant compared with 23.4±5.5% for controls. Likewise, the area of Trap staining for osteoclasts in POCs as a percentage of total staining in perichondrium and POC combined was 27.7±8.5% for mutant compared with 53.6±17.2% in controls. This is consistent with published findings that

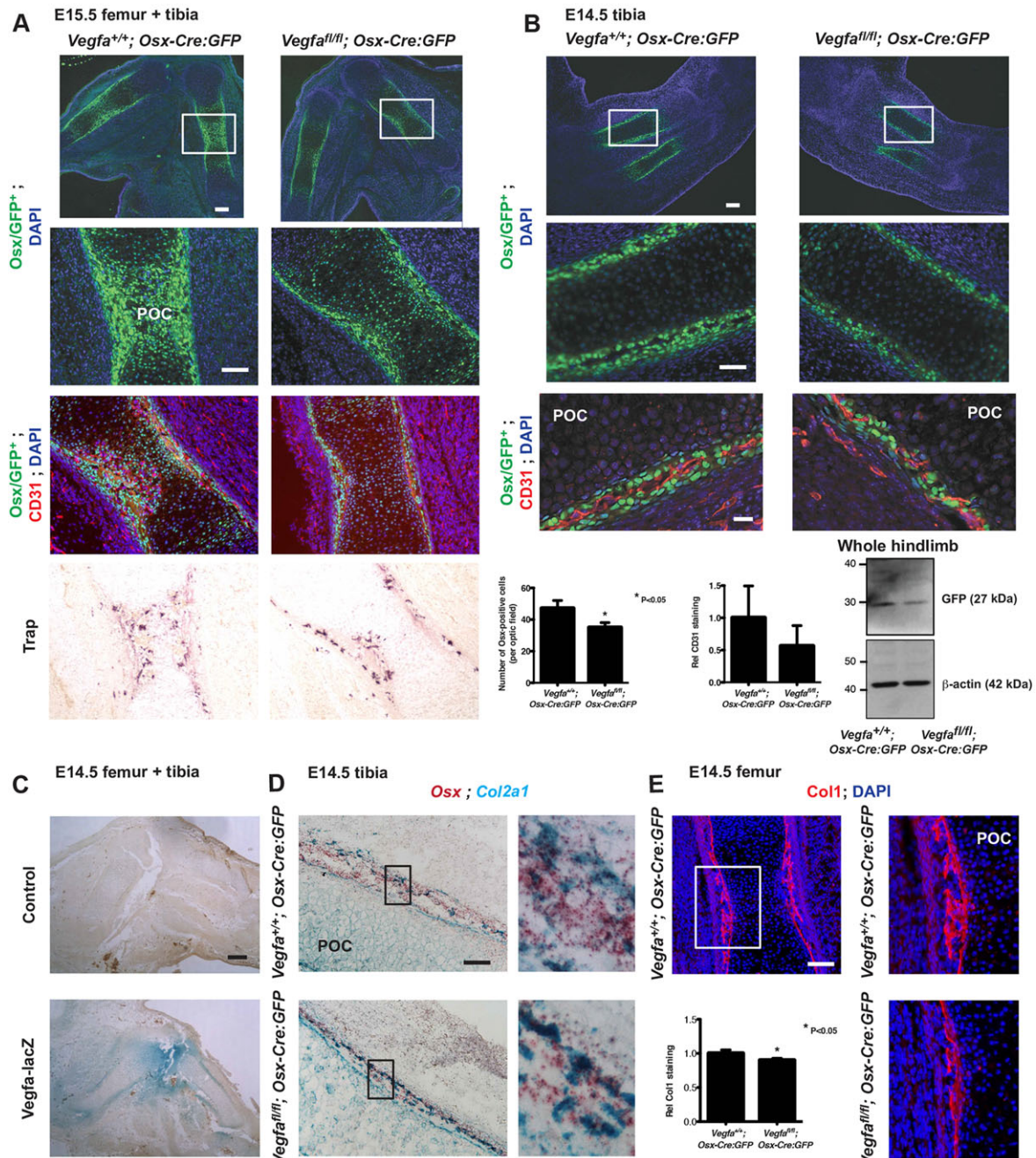


Fig. 2. Loss of Vegfa expression in osteolineage cells decreases perichondrial vascularity and osteoblast precursor numbers. (A) Osx/GFP⁺ cells (green) in E15.5 Vegfa^{+/+}; Osx-Cre:GFP (top left) and Vegfa^{fl/fl}; Osx-Cre:GFP (top right) femur and tibia sections (scale bar: 200 µm). The boxed femoral areas are magnified beneath (scale bar: 100 µm), showing anti-CD31 and Trap staining. (B) Osx/GFP⁺ cells in E14.5 Vegfa^{+/+}; Osx-Cre:GFP (top left) and Vegfa^{fl/fl}; Osx-Cre:GFP (top right) tibia and fibula sections (scale bar: 200 µm). Beneath are magnified views of the tibia areas boxed above (scale bar: 50 µm) and anti-CD31 staining of perichondrial areas (scale bar: 25 µm). Bar charts show quantification of Osx/GFP⁺ cells in the optic field and quantification of anti-CD31 staining in perichondrial areas of E14.5 tibia of Vegfa^{+/+}; Osx-Cre:GFP ($n=3$) and Vegfa^{fl/fl}; Osx-Cre:GFP ($n=3$) mice. Values represent the mean number of Osx/GFP⁺ cells per optic field or mean relative anti-CD31 staining \pm s.d. * $P<0.05$ for comparison between genotypes. The western blot is of GFP in E14.5 Vegfa^{+/+}; Osx-Cre:GFP and Vegfa^{fl/fl}; Osx-Cre:GFP whole hindlimb lysates. β -actin provides a loading control. (C) LacZ staining indicating Vegfa-expressing cells in femur and tibia sections from E14.5 Vegfa-lacZ mice as compared with WT control tissue (scale bar: 500 µm). (D) In situ hybridization on tibia sections of E14.5 Vegfa^{+/+}; Osx-Cre:GFP and Vegfa^{fl/fl}; Osx-Cre:GFP mice for Osx (red) and Col2a1 (turquoise) (scale bar: 50 µm). To the right are magnified views of the boxed perichondrial areas showing cells co-expressing Osx and Col2a1. (E) (Top left) Anti-Col1 staining of femur sections from E14.5 Vegfa^{+/+}; Osx-Cre:GFP mice (scale bar: 100 µm). (Bottom left) Quantification of Col1 staining of femur sections from Vegfa^{+/+}; Osx-Cre:GFP ($n=3$) and Vegfa^{fl/fl}; Osx-Cre:GFP ($n=3$) mice. Values represent mean relative staining area \pm s.d. * $P<0.05$ for comparison between genotypes. (Right) Magnified views of the boxed area of WT control and Vegfa^{fl/fl}; Osx-Cre:GFP mice.

Vegfa derived from Osx⁺ prehypertrophic chondrocytes attracts these cells into POCs (Maes et al., 2010b; Zelzer et al., 2002, 2004).

Loss of Vegfa expression in Osx⁺ cells resulted in decreased numbers of Osx/GFP⁺ cells in the perichondrial region of E14.5 tibia and reduced GFP levels in the whole hindlimb as assessed by

western blotting. Area of anti-CD31 staining indicated reduced, but not significant, differences in the perichondrium of mutant tibia (Fig. 2B), whereas the area of anti-CD34 staining, a marker of hematopoietic/endothelial cells, was reduced (supplementary material Fig. S2A). This suggests that reduced perichondrial vascularity might contribute to the decreased numbers of Osx/GFP⁺ cells. BrdU and TUNEL stainings confirmed that proliferating and apoptotic cell numbers were unaffected in E14.5 *Vegfa*^{fl/fl}; *Osx-Cre:GFP* mice (supplementary material Fig. S2B,C).

X-gal staining of hindlimbs of E14.5 *Vegfa*-lacZ mice indicated that perichondrial cells of tibia and femur express *Vegfa* (Fig. 2C; supplementary material Fig. S2D). No false-positive cells were observed in the control, as osteoclasts are hardly present (supplementary material Fig. S2E). At E14.5, the perichondrium contains specific pools of osteoblast lineage cells, including osteochondroprogenitors ($Col2^+$), osteoblast precursors (Osx^+) and mature osteoblasts ($Col1^+$) (Maes et al., 2010b). *In situ* hybridization confirmed co-expression of *Osx* and *Col2* (*Col2a1*) in perichondrial cells (Fig. 2D), and perichondrial osteochondroprogenitors and their progeny were present in mice carrying *Tomato* and *Col2-Cre* transgenes (supplementary material Fig. S2F).

Next, we compared mice carrying floxed *Vegfa* alleles and *Osx-Cre:GFP* or *Col2-Cre* transgenes. Loss of *Vegfa* expression in *Osx-GFP*⁺ cells in *Vegfa*^{fl/fl}; *Osx-Cre:GFP* mice was confirmed by *in situ* hybridization (supplementary material Fig. S2G). *Osx* expression was reduced and *Col2* expression appeared increased in tibia sections of E14.5 mutant mice (Fig. 2D), suggesting reduced differentiation of $Col2^+$ osteochondroprogenitors into Osx^+ cells. Probing sections for *Col1* mRNA (supplementary material Fig. S2H) or *Col1* protein revealed that loss of *Vegfa* in *Osx-GFP*⁺ cells or $Col2^+$ cells resulted in slightly reduced *Col1* expression in perichondrial areas (Fig. 2E; supplementary material Fig. S2I). Thus, *Vegfa* produced by $Col2^+$ and Osx^+ osteoprogenitors appears to primarily function as a stimulator of osteolineage differentiation.

Vegfa stimulates Vegfr2 signaling and β -catenin expression

Most effects of *Vegfa* are mediated by Vegfr1 (Flt1 – Mouse Genome Informatics) and Vegfr2 (Kdr – Mouse Genome Informatics; also known as Flk1) (Ferrara et al., 2003). Vegfr2 regulates chemotaxis, mitogenesis and cytoskeletal reorganization (Carmeliet and Collen, 1999); Vegfr1 primarily acts as a decoy receptor, although its function depends on the developmental stage (Ferrara et al., 2003). Overexpression of *Vegfa* in $Col2^+$ osteochondroprogenitors enhances bone mass by mechanisms involving Vegfr2 and β -catenin pathways (Maes et al., 2010a). Staining tibia sections of E14.5 *Vegfa*^{+/+}; *Osx-Cre:GFP* mice with anti-Vegfr2 indicated abundant Vegfr2 expression in perichondrial *Osx-GFP*⁺ and likely $Col2^+$ cells (Fig. 3A).

Conditional deletion of *Vegfr2* in *Vegfr2*^{fl/fl}; *Osx-Cre:GFP* mice resulted in reduced numbers of *Osx-GFP*⁺ cells (Fig. 3A). *Col1* levels appeared reduced in the perichondrium of *Vegfr2*^{fl/fl}; *Osx-Cre:GFP* (Fig. 3B) and *Vegfr2*^{fl/fl}; *Col2-Cre:GFP* mice (supplementary material Fig. S3A). Perichondrial regions of E14.5 femurs from *Vegfr2*^{fl/fl}; *Tomato*; *Col2-Cre* and *Vegfr2*^{+/+}; *Tomato*; *Col2-Cre* mice had similar numbers of *Tomato*-positive cells (supplementary material Fig. S3B). Therefore, *Vegfa*-dependent control of differentiation early in the osteoblast lineage appears to be mediated by Vegfr2. Vegfr1 is also abundantly expressed in perichondrial cells; however, conditional deletion of

this receptor in osteoblast lineage cells had no clear effect on the numbers of *Osx*/GFP⁺ cells and *Col1* levels in the perichondrium of E14.5 tibia (supplementary material Fig. S3C,D). Newborn *Vegfa*^{fl/fl}; *Osx-Cre:GFP* and *Vegfr2*^{fl/fl}; *Osx-Cre:GFP* mice had no apparent defects compared with their littermate controls (supplementary material Fig. S3E).

Phosphorylation of Vegfr2, Akt and Gsk3 β in hindlimb lysates of E14.5 *Vegfa*^{fl/fl}; *Osx-Cre:GFP* was decreased, whereas Mapk phosphorylation was unaffected (Fig. 3C). Furthermore, loss of *Vegfa* or Vegfr2 in *Osx*⁺ cells resulted in reduced β -catenin expression. Anti- β -catenin staining of tibia sections confirmed reduced β -catenin expression in perichondrial cells (Fig. 3D). Thus, *Vegfa*-induced Vegfr2 signaling and possibly also the β -catenin pathway regulate osteoblast differentiation in the perichondrium of developing bones.

Vegfa stimulates Ihh expression and represses Notch2 levels

Apart from Wnt/ β -catenin, several other factors regulate endochondral osteoblast differentiation, including Bmps, Fgfs, PthrP, Ihh (Colnot et al., 2005; Hu et al., 2005; Razzaque et al., 2005) and Notch2 (Hilton et al., 2008). To assess possible roles in *Vegfa*-dependent control of differentiation, we analyzed Ihh and Notch2 expression in hindlimb lysates from E14.5 *Vegfa*^{fl/fl}; *Osx-Cre:GFP* and *Vegfr2*^{fl/fl}; *Osx-Cre:GFP* mice. Loss of *Vegfa* or Vegfr2 in *Osx*⁺ cells resulted in decreased Ihh expression but increased Notch2 (Fig. 4A). *Ihh* is expressed in prehypertrophic chondrocytes and cells located in perichondrium during endochondral ossification (Hu et al., 2005; Mak et al., 2006). *In situ* hybridization of tibia sections from *Vegfa*^{fl/fl}; *Osx-Cre:GFP* and *Vegfa*^{+/+}; *Osx-Cre:GFP* mice indicated that *Ihh* expression was reduced in prehypertrophic mutant chondrocytes (Fig. 4B), whereas no *Ihh* expression was detected in mutant and control perichondrial cells (supplementary material Fig. S4A). Thus, reduced *Ihh* expression in prehypertrophic chondrocytes might directly affect osteoblast differentiation during perichondrial maturation. Anti-Notch2 staining of tibia sections showed increased Notch2 expression in perichondrial cells of mutants (Fig. 4C). These data suggest functional links between *Vegfa*/Vegfr2, Ihh and Notch2 in perichondrial osteoblast differentiation.

To test whether *Vegfa* directly regulates the expression of *Ihh* and *Notch2*, we used hindlimb cells from E13.5 *Vegfa*^{fl/fl} mice for *in vitro* differentiation assays. The majority of *Vegfa*-expressing cells showed nuclear *Osx* expression (Fig. 4Da). Adenoviral Cre-mediated *Vegfa* knockdown was confirmed by measuring cell-associated and secreted *Vegfa* levels (supplementary material Fig. S4Ba). Expression of the early and late osteoblast marker genes *Runx2*, *Osx* (*Sp7*) and *Colla1*, and the mRNA levels of *Ihh* and the *Ihh* target genes *Patched 1* (*Ptch1*), *Gli1* and hedgehog interacting protein (*Hhip*) were reduced upon loss of *Vegfa* expression (Fig. 4Db,c). Expression of *Notch2* and target gene hairy/enhancer-of-split related with YRPW motif 1 (*Hey1*) was unaffected (supplementary material Fig. S4Bb), suggesting the possibility that cell-cell contact *in vivo* is important for regulation of *Notch2* expression by *Vegfa*.

In rescue experiments, *Osx* expression was eliminated in the presence of the hedgehog (*Hh*) antagonist GANT-58, whereas recombinant *Vegfa* had only minor effects and *Runx2* and *Colla1* levels were not affected (Fig. 4Dd). This raises the possibility that *Vegfa* might require one or more co-factors to exert its effect on osteoblast differentiation; alternatively, *Vegfa* functions via intracrine rather than paracrine mechanisms, as described in

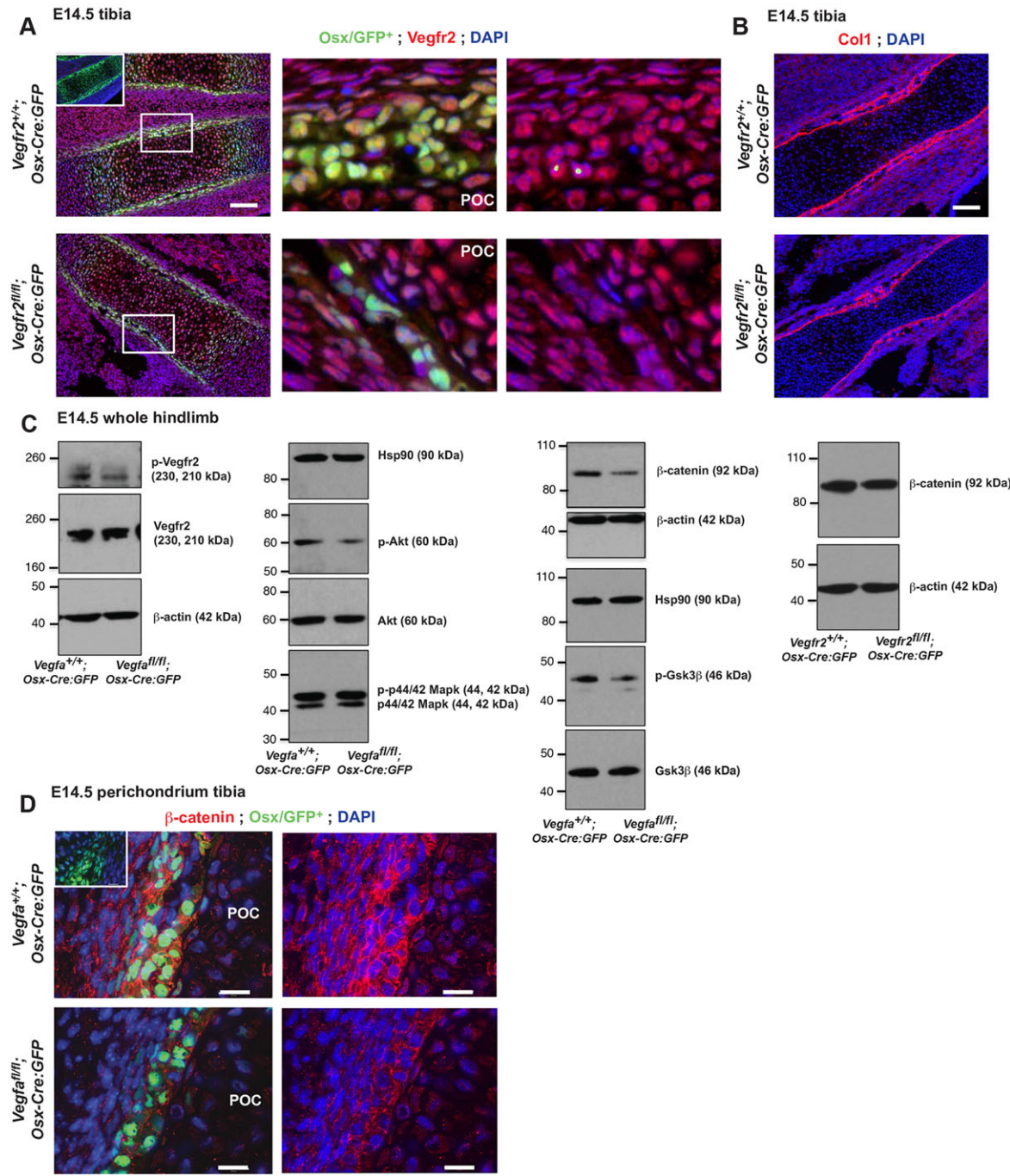


Fig. 3. Loss of Vegfr2 in osteoprogenitors results in reduced osteoblast differentiation and loss of Vegfa/Vegfr2 signaling reduces β-catenin expression in perichondrial cells. (A) (Left) Anti-Vegfr2 staining of tibia sections from E14.5 *Vegfr2^{+/+;} Osx-Cre:GFP* and *Vegfr2^{fl/fl;} Osx-Cre:GFP* mice (scale bar: 100 μm); inset shows non-immune IgG control. Boxed regions are magnified to the right, showing *Osx/GFP⁺* cells (green, middle column) or Vegfr2 staining only (right column). (B) Anti-Col1 staining of tibia sections from E14.5 *Vegfr2^{+/+;} Osx-Cre:GFP* and *Vegfr2^{fl/fl;} Osx-Cre:GFP* mice (scale bar: 100 μm). (C) Western blotting of phospho-Vegfr2 (Tyr1175), phospho-Akt (Ser473), phospho-p44/42 Mapk (Mapk3/1) (Thr202/Tyr204), β-catenin and phospho-Gsk3β (Ser9) protein levels in whole hindlimb lysates from E14.5 *Vegfa^{+/+;} Osx-Cre:GFP*, *Vegfa^{fl/fl;} Osx-Cre:GFP* and *Vegfr2^{fl/fl;} Osx-Cre:GFP* mice; β-actin and Hsp90 provide loading controls. (D) Anti-β-catenin staining of perichondrial area of tibia sections from E14.5 *Vegfa^{+/+;} Osx-Cre:GFP* and *Vegfa^{fl/fl;} Osx-Cre:GFP*; inset shows non-immune IgG control (scale bars: 20 μm). To the right is shown anti-β-catenin staining alone.

adult mice (Liu et al., 2012). We also tested the possible involvement of Gαs (Gnas – Mouse Genome Informatics), which is a modulator of Wnt/β-catenin and Hh signaling activities in mesenchymal progenitors (Regard et al., 2011, 2013). In hindlimb lysates, Gαs expression was not affected in *Vegfa^{fl/fl;} Osx-Cre:GFP* mice (supplementary material Fig. S4Ca). Furthermore, the activity of protein kinase A (Pka), a major

regulator of Hh signaling, was unaffected in these mice (supplementary material Fig. S4Cb).

In summary, our data demonstrate that Vegfa produced by *Osx⁺* precursors regulates blood vessel recruitment and early stages of osteoblast differentiation during perichondrial maturation. Vegfa-dependent effects are mediated by Vegfr2 and mechanisms that include stimulated expression and activity of Ihh, increased

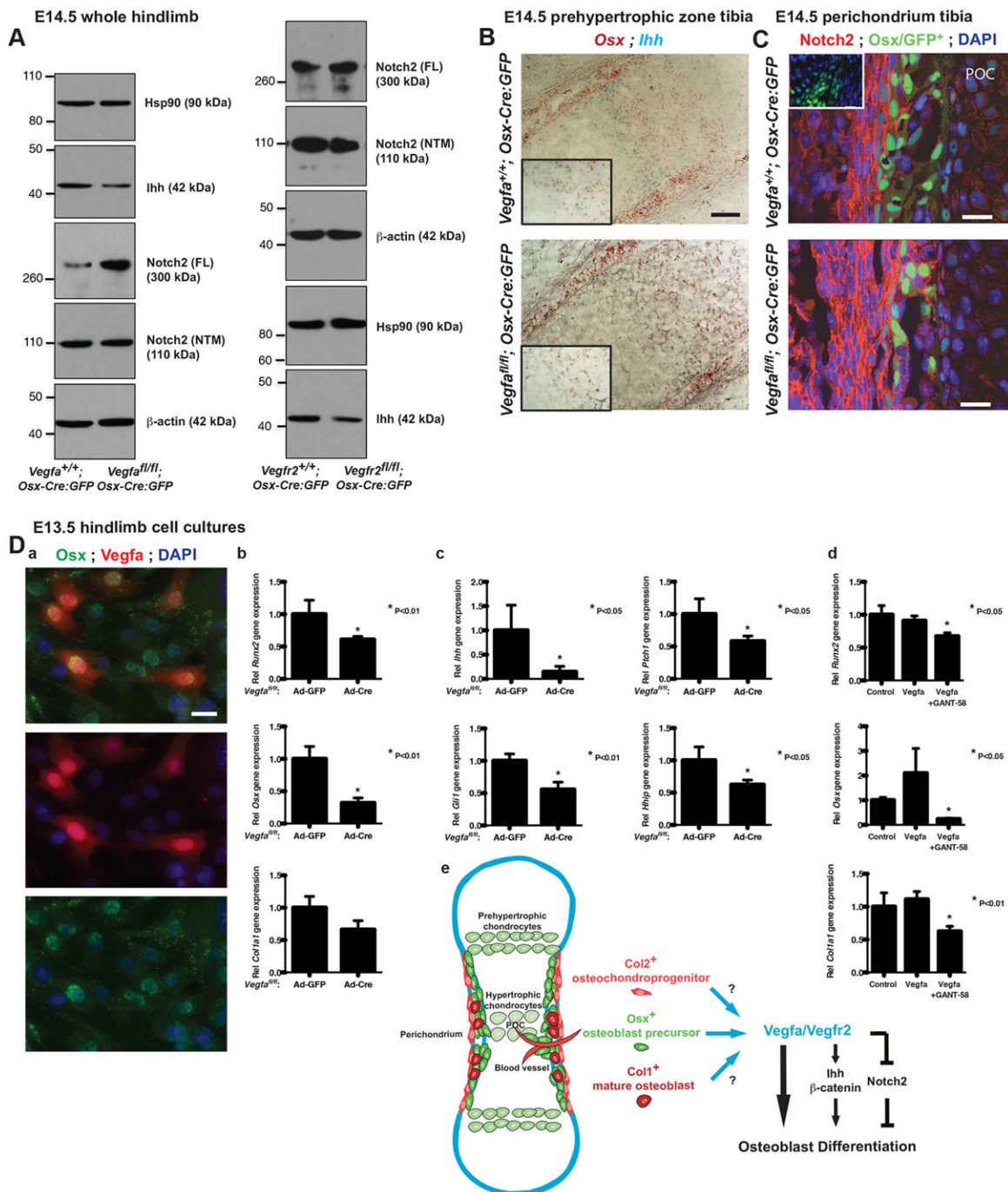


Fig. 4. Vegfa stimulates Ihh/Gli1 signaling and inhibits Notch2 expression in perichondrial cells. (A) Western blotting of Ihh and Notch2 in whole hindlimb lysates from E14.5 *Vegfa/Vegfr2^{+/+}; Osx-Cre:GFP*, *Vegfa^{fl/fl}; Osx-Cre:GFP* and *Vegfr2^{fl/fl}; Osx-Cre:GFP* mice; β -actin and Hsp90 are loading controls. (B) *In situ* hybridization of Osx (red) and Ihh (turquoise) on tibia sections (prehypertrophic zone region) from E14.5 *Vegfa^{+/+}; Osx-Cre:GFP* and *Vegfa^{fl/fl}; Osx-Cre:GFP* mice (scale bars: 50 μ m). Insets are magnified views of prehypertrophic chondrocyte areas. (C) Anti-Notch2 staining of perichondrial area of tibia sections from E14.5 *Vegfa^{+/+}; Osx-Cre:GFP* and *Vegfa^{fl/fl}; Osx-Cre:GFP* mice; inset shows non-immune IgG control (scale bars: 20 μ m). (D) (a) Anti-Vegfa and anti-Osx staining of cultured hindlimb cells from E13.5 *Vegfa^{fl/fl}* embryos (scale bar: 50 μ m). (b,c) Expression, as assessed by qRT-PCR, of *Runx2*, *Osx* (*Sp7*), *Col1a1*, *Ihh*, *Ptch1*, *Gli1* and *Hhip* in lysates of cultured hindlimb cells from E13.5 *Vegfa^{fl/fl}* embryos, treated with adenoviral Cre and induced to differentiate into osteoblasts. Control cells were treated with adenoviral GFP. Relative gene expression levels are normalized to levels of *Gapdh*. Values represent mean relative expression \pm s.d. ($n=3$). (d) Expression (by qRT-PCR) of *Runx2*, *Osx* (*Sp7*) and *Col1a1* in lysates of cultured hindlimb cells from E13.5 *Vegfa^{fl/fl}* embryos, treated with adenoviral Cre and induced to differentiate into osteoblasts in the presence of recombinant Vegfa with or without the Hh antagonist GANT-58, as compared with control cells. Relative gene expression levels were normalized to levels of *Gapdh*. Values represent mean relative expression \pm s.d. ($n=3$). (e) Model summarizing our findings and conclusions. During perichondrial maturation, Col2⁺ osteochondroprogenitors differentiate into Osx⁺ precursors, which either migrate into the POC in response to Vegfa secreted by (pre)hypertrophic chondrocytes or mature into Col1⁺ osteoblasts in the perichondrium. Vegfa derived from perichondrial osteolineage cells controls osteoblast differentiation in a Vegfr2-dependent manner, likely involving Ihh-, β -catenin- and Notch2-dependent pathways.

expression of β -catenin and inhibition of Notch2 (Fig. 4D). Since many factors are crucial for osteoblast differentiation during endochondral bone formation, Vegfa/Vegfr2-dependent regulation of osteoblast differentiation might involve additional mechanisms as well. Furthermore, in addition to an autocrine/paracrine role of Vegfa, changes in perichondrial vascularity indicative of a general developmental delay might also contribute to the effects on osteoblast differentiation.

MATERIALS AND METHODS

Mouse strains

Floxed *Vegfa*, *Vegfr2* (*Flk1*) and *Vegfr1* (*Flt1*) mice were generated at Genentech. 129-*Vegfam1.1Nagy* (Miquerol et al., 1999), *Osx-Cre:GFP* (Rodda and McMahon, 2006) and *Col2-Cre* (Schipani et al., 2001) mice have been described previously. B6.Cg-*Gt(ROSA)26Sortm1(CAG-tdTomato)Hze/J* mice were purchased from Jackson Laboratory. All animal experiments were performed with protocols approved by Harvard Medical Area Standing Committee on Animals and in accordance with US Public Health Service Policy on Humane Care and Use of Laboratory Animals. Further details of mouse strains and genotyping are provided in the supplementary Materials and Methods and Table S1.

Staining, histology and microCT

Alizarin Red and Alcian Blue staining of skeletal structures in P1 mice and microCT analyses on hindlimbs are described in the supplementary Materials and Methods. Frozen sections (7.5 μ m) were prepared for histology, including Hematoxylin and Eosin (H&E), von Kossa and Trap staining, and analyzed with a Nikon 80i upright microscope or a Nikon Ti w/ spinning disk confocal microscope as described in the supplementary Materials and Methods. X-Gal staining to detect *Vegfa-lacZ* expression, and BrdU and TUNEL staining of proliferating and apoptotic cells are detailed in the supplementary Materials and Methods.

Immunohistochemistry (IHC), immunocytochemistry (ICH) and western blotting

IHC on frozen limb sections, ICH on fixed cells in culture chambers and western blotting of protein lysates of E14.5 hindlimbs were carried out with the antibodies and imaging techniques described in the supplementary Materials and Methods.

ELISA

Vegfa protein levels in cell lysates (cell associated) or culture medium (secreted) were assessed and normalized as described in the supplementary Materials and Methods.

RNA *in situ* hybridization and qRT-PCR

Gene expression analyses by RNA *in situ* hybridization and qRT-PCR were carried out using the probes and primers detailed in the supplementary Materials and Methods and Table S2.

Mesenchymal progenitor cell cultures

Hindlimbs of E13.5 embryos were enzymatically digested and cells infected with either Ad-Cre or Ad-GFP followed by osteogenic induction as described in the supplementary Materials and Methods.

Quantifications and statistical analysis

Quantifications of femur diameter, mineralization and cell counts (*Osx*, Trap, CD31, CD34 and *Col1* staining) were performed as described in the supplementary Materials and Methods. Results are presented as mean \pm s.d. and unpaired Student's *t*-tests were used. $P<0.05$ was considered significant.

Acknowledgements

We thank Yulia Pittel for secretarial assistance; Sofiya Plotkina and Karen Cox for technical support; Andras Nagy (Lunenfeld-Tanenbaum Research Institute, Canada) for providing Vegfa-lacZ mice; Napoleone Ferrara (UC San Diego) and

Genentech for providing mice with floxed *Vegfa*, *Flk1* and *Flt1* alleles; Beate Lanske (HSDM) for providing *Col2-Cre* mice; and Valerie Salazar (HSDM) for advice on X-gal staining. We acknowledge services of the MicroCT Core at HSDM and Nikon Imaging Center at HMS.

Competing interests

The authors declare no competing or financial interests.

Author contributions

X.D., B.R.O. and A.D.B. designed experiments and interpreted results. X.D., Y.M., Y.L., C.N. and A.D.B. performed the experiments. X.D., B.R.O. and A.D.B. wrote the manuscript.

Funding

This work was supported by the National Institutes of Health [grants AR36819, AR36820 and AR48564 to B.R.O.] and partially supported by an HSDM Dean's Scholarship (to A.D.B.). Deposited in PMC for release after 12 months.

Supplementary material

Supplementary material available online at <http://dev.biologists.org/lookup/suppl/doi:10.1242/dev.117952/-DC1>

References

- Carmeliet, P. and Collen, D. (1999). Role of vascular endothelial growth factor and vascular endothelial growth factor receptors in vascular development. *Curr. Top. Microbiol. Immunol.* **237**, 133-158.
- Chung, U.-i., Schipani, E., McMahon, A. P. and Kronenberg, H. M. (2001). Indian hedgehog couples chondrogenesis to osteogenesis in endochondral bone development. *J. Clin. Invest.* **107**, 295-304.
- Colnot, C., de la Fuente, L., Huang, S., Hu, D., Lu, C., St-Jacques, B. and Helms, J. A. (2005). Indian hedgehog synchronizes skeletal angiogenesis and perichondrial maturation with cartilage development. *Development* **132**, 1057-1067.
- Day, T. F., Guo, X., Garrett-Beal, L. and Yang, Y. (2005). Wnt/beta-catenin signaling in mesenchymal progenitors controls osteoblast and chondrocyte differentiation during vertebrate skeletogenesis. *Dev. Cell* **8**, 739-750.
- Ferrara, N., Gerber, H.-P. and LeCouter, J. (2003). The biology of VEGF and its receptors. *Nat. Med.* **9**, 669-676.
- Haigh, J. J., Gerber, H. P., Ferrara, N. and Wagner, E. F. (2000). Conditional inactivation of VEGF-A in areas of collagen2a1 expression results in embryonic lethality in the heterozygous state. *Development* **127**, 1445-1453.
- Hill, T. P., Später, D., Taketo, M. M., Birchmeier, W. and Hartmann, C. (2005). Canonical Wnt/beta-catenin signaling prevents osteoblasts from differentiating into chondrocytes. *Dev. Cell* **8**, 727-738.
- Hilton, M. J., Tu, X., Wu, X., Bai, S., Zhao, H., Kobayashi, T., Kronenberg, H. M., Teitelbaum, S. L., Ross, F. P., Kopan, R. et al. (2008). Notch signaling maintains bone marrow mesenchymal progenitors by suppressing osteoblast differentiation. *Nat. Med.* **14**, 306-314.
- Hu, H., Hilton, M. J., Tu, X., Yu, K., Ornitz, D. M. and Long, F. (2005). Sequential roles of Hedgehog and Wnt signaling in osteoblast development. *Development* **132**, 49-60.
- Karsenty, G. (2003). The complexities of skeletal biology. *Nature* **423**, 316-318.
- Karsenty, G. and Wagner, E. F. (2002). Reaching a genetic and molecular understanding of skeletal development. *Dev. Cell* **2**, 389-406.
- Kronenberg, H. M. (2003). Developmental regulation of the growth plate. *Nature* **423**, 332-336.
- Liu, Y., Berendsen, A. D., Jia, S., Lotinun, S., Baron, R., Ferrara, N. and Olsen, B. R. (2012). Intracellular VEGF regulates the balance between osteoblast and adipocyte differentiation. *J. Clin. Invest.* **122**, 3101-3113.
- Long, F., Chung, U. I., Ohba, S., McMahon, J., Kronenberg, H. M. and McMahon, A. P. (2004). Ihh signaling is directly required for the osteoblast lineage in the endochondral skeleton. *Development* **131**, 1309-1318.
- Maes, C., Carmeliet, P., Moermans, K., Stockmans, I., Smets, N., Collen, D., Bouillon, R. and Carmeliet, G. (2002). Impaired angiogenesis and endochondral bone formation in mice lacking the vascular endothelial growth factor isoforms VEGF164 and VEGF188. *Mech. Dev.* **111**, 61-73.
- Maes, C., Goossens, S., Bartunkova, S., Drogat, B., Coenegrachts, L., Stockmans, I., Moermans, K., Nyabi, O., Haigh, K., Naessens, M. et al. (2010a). Increased skeletal VEGF enhances beta-catenin activity and results in excessively ossified bones. *EMBO J.* **29**, 424-441.
- Maes, C., Kobayashi, T., Selig, M. K., Torrekens, S., Roth, S. I., Mackem, S., Carmeliet, G. and Kronenberg, H. M. (2010b). Osteoblast precursors, but not mature osteoblasts, move into developing and fractured bones along with invading blood vessels. *Dev. Cell* **19**, 329-344.
- Mak, K. K., Chen, M.-H., Day, T. F., Chuang, P.-T. and Yang, Y. (2006). Wnt/beta-catenin signaling interacts differentially with Ihh signaling in controlling endochondral bone and synovial joint formation. *Development* **133**, 3695-3707.

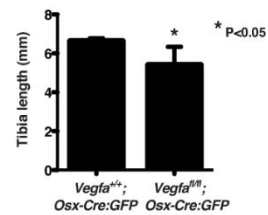
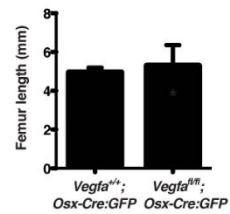
- Miquerol, L., Gertsenstein, M., Harpal, K., Rossant, J. and Nagy, A.** (1999). Multiple developmental roles of VEGF suggested by a LacZ-tagged allele. *Dev. Biol.* **212**, 307-322.
- Nakashima, K., Zhou, X., Kunkel, G., Zhang, Z., Deng, J. M., Behringer, R. R. and de Crombrugghe, B.** (2002). The novel zinc finger-containing transcription factor osterix is required for osteoblast differentiation and bone formation. *Cell* **108**, 17-29.
- Razzaque, M. S., Soegiarto, D. W., Chang, D., Long, F. and Lanske, B.** (2005). Conditional deletion of Indian hedgehog from collagen type 2alpha1-expressing cells results in abnormal endochondral bone formation. *J. Pathol.* **207**, 453-461.
- Regard, J. B., Cherman, N., Palmer, D., Kuznetsov, S. A., Celi, F. S., Guettier, J.-M., Chen, M., Bhattacharya, N., Wess, J., Coughlin, S. R. et al.** (2011). Wnt/beta-catenin signaling is differentially regulated by Galphai proteins and contributes to fibrous dysplasia. *Proc. Natl. Acad. Sci. USA* **108**, 20101-20106.
- Regard, J. B., Malhotra, D., Gvozdenovic-Jeremic, J., Josey, M., Chen, M., Weinstein, L. S., Lu, J., Shore, E. M., Kaplan, F. S. and Yang, Y.** (2013). Activation of Hedgehog signaling by loss of GNAS causes heterotopic ossification. *Nat. Med.* **19**, 1505-1512.
- Rodda, S. J. and McMahon, A. P.** (2006). Distinct roles for Hedgehog and canonical Wnt signaling in specification, differentiation and maintenance of osteoblast progenitors. *Development* **133**, 3231-3244.
- Schipani, E., Ryan, H. E., Didrickson, S., Kobayashi, T., Knight, M. and Johnson, R. S.** (2001). Hypoxia in cartilage: HIF-1alpha is essential for chondrocyte growth arrest and survival. *Genes. Dev.* **15**, 2865-2876.
- Zelzer, E. and Olsen, B. R.** (2003). The genetic basis for skeletal diseases. *Nature* **423**, 343-348.
- Zelzer, E., McLean, W., Ng, Y. S., Fukai, N., Reginato, A. M., Lovejoy, S., D'Amore, P. A. and Olsen, B. R.** (2002). Skeletal defects in VEGF(120/120) mice reveal multiple roles for VEGF in skeletogenesis. *Development* **129**, 1893-1904.
- Zelzer, E., Mamluk, R., Ferrara, N., Johnson, R. S., Schipani, E. and Olsen, B. R.** (2004). VEGFA is necessary for chondrocyte survival during bone development. *Development* **131**, 2161-2171.

A P9 femur + tibia

Vegfa^{+/+}; Osx-Cre:GFP



Vegfa^{fl/fl}; Osx-Cre:GFP



B P1 femur

Control



Vegfa-LacZ

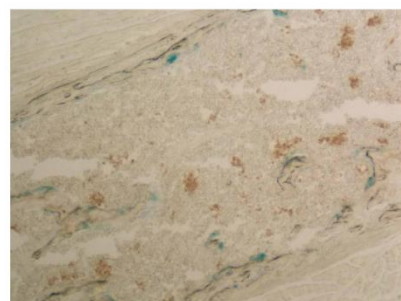


Fig. S1. Progenitor-derived Vegfa regulates the length of early postnatal tibia.

(A) Micro-CT 3D scans of hindlimbs from P9 *Vegfa^{+/+}; Osx-Cre:GFP* (control, left) and *Vegfa^{fl/fl}; Osx-Cre:GFP* (mutant, middle) mice. Graphs: Quantification of femur length (mm) (upper right) and tibia length (mm) (lower right) of P9 *Vegfa^{+/+}; Osx-Cre:GFP* (n=4) and *Vegfa^{fl/fl}; Osx-Cre:GFP* (n=5) mice. Values represent mean length measures \pm s.d.. P<0.05 for comparison between genotypes. Note that because of the variable bending between the femur and tibia, the two-dimensional projection as shown here does not constitute the measures of the length of the bones. (B) LacZ staining indicating *Vegfa*-expressing cells in P1 femur of *Vegfa-lacZ* mice (right) compared with WT control tissue (left) (scale bar: 200 μ m). Bottom: Magnified views of POC and prehypertrophic areas of femoral areas showing *Vegfa*-positive cells (arrows).

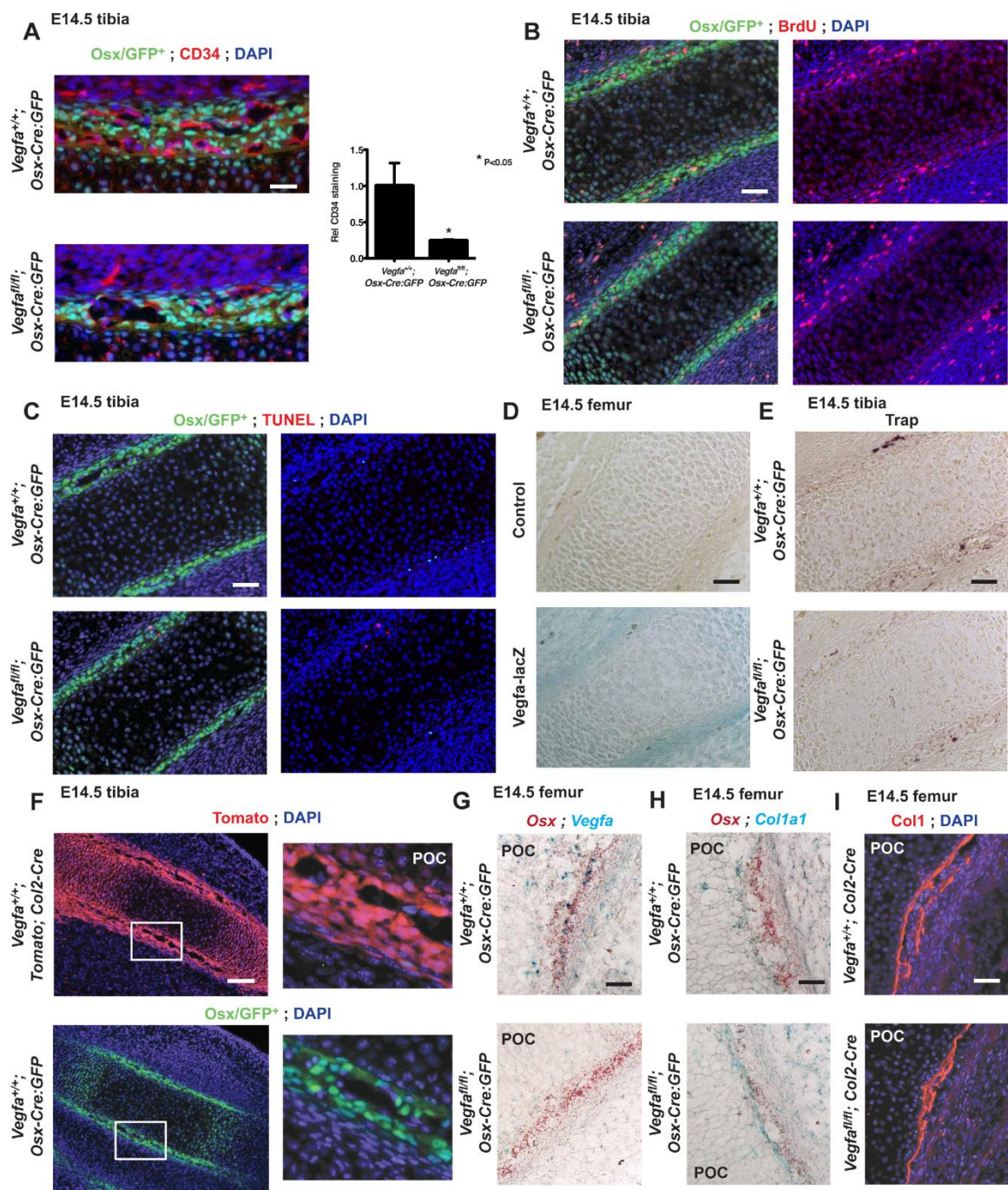


Fig. S2. Loss of progenitor-derived Vegfa does not affect the proliferation and apoptosis of Osx⁺ cells in perichondrial areas.

(A) Anti-CD34 staining of perichondrial areas of tibia sections of *Vegfa^{+/+}; Osx-Cre:GFP* and *Vegfa^{fl/fl}; Osx-Cre:GFP* mice (scale bar: 25 μ m). Right: Quantification of anti-CD34 staining in perichondrium of E14.5 tibia of *Vegfa^{+/+}; Osx-Cre:GFP* (n=3) and *Vegfa^{fl/fl}; Osx-Cre:GFP* (n=3) mice. Values represent mean relative anti-CD34 staining \pm s.d.. P<0.05 for comparison between genotypes. (B) BrdU staining of tibia sections from E14.5 *Vegfa^{+/+}; Osx-Cre:GFP* (top) and *Vegfa^{fl/fl}; Osx-Cre:GFP* (bottom) mice showing Osx/GFP⁺ cells in perichondrial areas of tibia (scale bar: 50 μ m). Right: Identical images showing BrdU staining only. (C) TUNEL staining of tibia sections from E14.5 *Vegfa^{+/+}; Osx-Cre:GFP* (top) and *Vegfa^{fl/fl}; Osx-Cre:GFP* (bottom) mice showing Osx/GFP⁺ cells in perichondrial areas of tibia (scale bar: 50 μ m). Right: Identical images showing TUNEL staining only. (D) LacZ staining indicating *Vegfa*-expressing cells in E14.5 femur of *Vegfa-LacZ* mice (bottom) compared to no background staining in tissue from WT control mice (top) (scale bar: 50 μ m). (E) Trap staining of tibia sections from E14.5 *Vegfa^{+/+}; Osx-Cre:GFP* (top) and *Vegfa^{fl/fl}; Osx-Cre:GFP* (bottom) mice showing osteoclasts in perichondrial areas of tibia (scale bar: 50 μ m). (F) Analysis of different cell populations located in perichondrium of E14.5 tibia. Top: Tibia section from E14.5 *Vegfa^{+/+}; Tomato; Col2-Cre* mice showing cells derived from osteochondroprogenitor (Col2⁺) cells (scale bar: 100 μ m). Bottom: Tibia from *Vegfa^{+/+}; Osx-Cre:GFP* mice showing Osx-expressing cells. Right: Magnified views of delineated rectangular areas of perichondrium in images on left. (G) *In situ* hybridization on femur sections of E14.5 *Vegfa^{+/+}; Osx-Cre:GFP* (top) and *Vegfa^{fl/fl}; Osx-Cre:GFP* (bottom) mice for *Osx* (red spots) and *Vegfa* (turquoise spots) (scale bar: 50 μ m). (H) *In situ* hybridization on femur sections of E14.5 *Vegfa^{+/+}; Osx-Cre:GFP* (top) and *Vegfa^{fl/fl}; Osx-Cre:GFP* (bottom) mice for *Osx* (red spots) and *Colla1* (turquoise spots) (scale bar: 50 μ m). (I) Anti-Coll1 staining of

femur sections from E14.5 *Vegfa^{fl/fl}; Col2-Cre* (bottom) and WT control (top) mice showing Col1 deposition in perichondrial area at center of femur (scale bar: 50 μm).

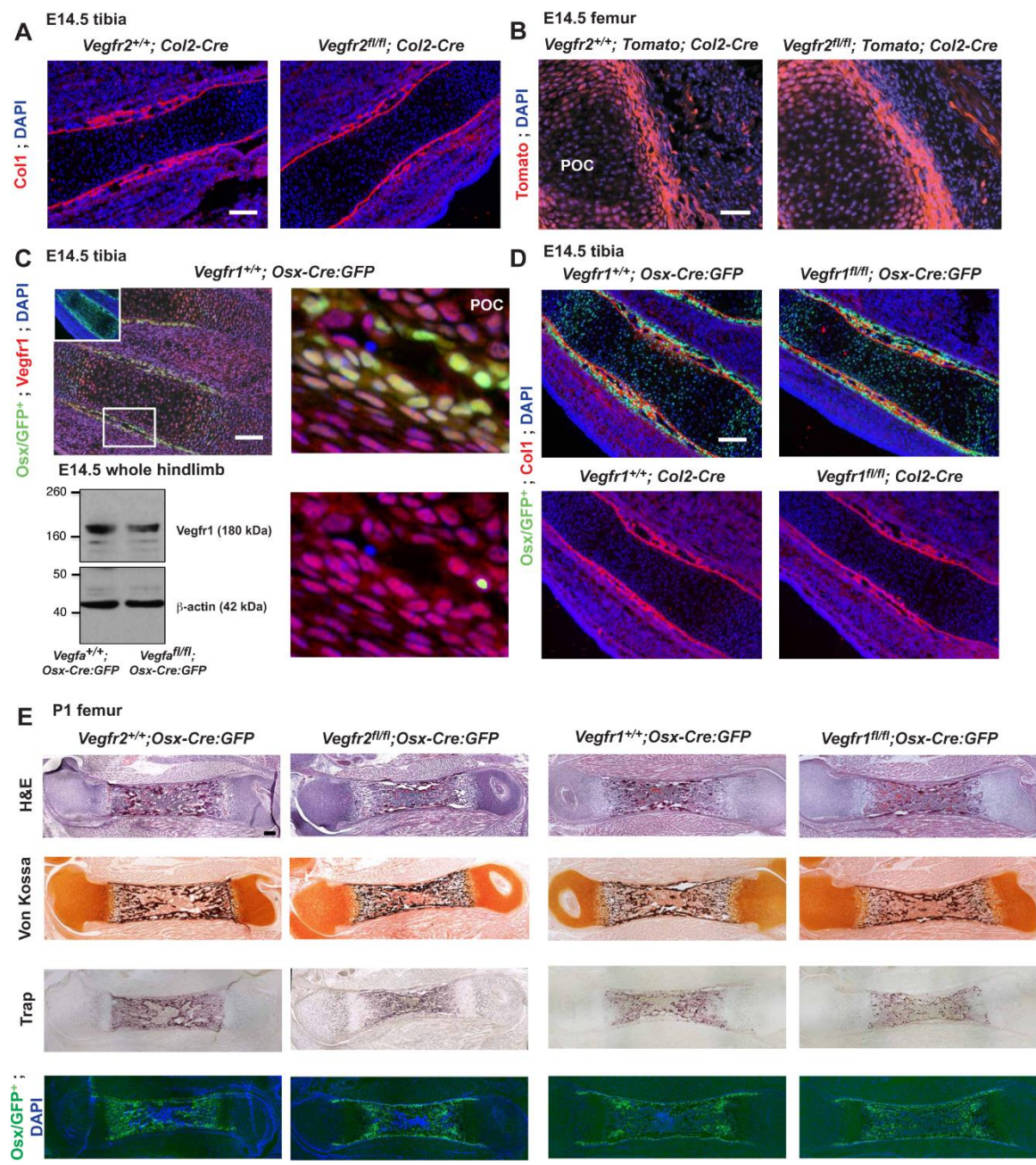


Fig. S3. Loss of Vegfr1 in osteoprogenitor cells does not affect osteoblast differentiation in perichondrium and mineralization of developing bones.

(A) Anti-Col1 staining of tibia sections from E14.5 *Vegfr2^{+/+}; Col2-Cre* (left) and *Vegfr2^{f/f}; Col2-Cre* (right) mice (scale bar: 100 μ m). (B) Femur sections from E14.5 *Vegfr2^{+/+}; Tomato; Col2-Cre* (left) and *Vegfr2^{f/f}; Tomato; Col2-Cre* (right) mice showing cells derived from osteochondroprogenitor ($Col2^+$) cells (scale bar: 50 μ m). (C) Top left: Anti-Vegfr1 staining of tibia sections from E14.5 *Vegfr1^{+/+}; Osx-Cre:GFP* mice showing Osx/GFP⁺ cells in the perichondrium with insert showing non-immune IgG control (scale bar: 100 μ m). Top right: Magnified view of delineated rectangular area at left showing Osx/GFP⁺ cells (green) and identical images with Vegfr1 staining only (bottom right). Bottom left: Western blotting of Vegfr1 protein levels in whole hindlimb lysates from E14.5 *Vegfa^{+/+}; Osx-Cre:GFP* (control) and *Vegfa^{f/f}; Osx-Cre:GFP* (mutant) mice; β -actin is loading control. (D) Anti-Col1 staining of femur sections from E14.5 *Vegfr1^{+/+}; Osx-Cre:GFP* (top left) and *Vegfr1^{f/f}; Osx-Cre:GFP* (top right) and femur sections from *Vegfr1^{+/+}; Col2-Cre* (bottom left) and *Vegfr1^{f/f}; Col2-Cre* (bottom right) mice (scale bar: 100 μ m). (E) Histological analysis of femur sections from P1 *Vegfr2^{f/f}; Osx-Cre:GFP* (left) and *Vegfr1^{f/f}; Osx-Cre:GFP* (right) compared to WT littermate control mice by H&E, Von Kossa, Trap and Osx/GFP⁺ expression (scale bar: 200 μ m).

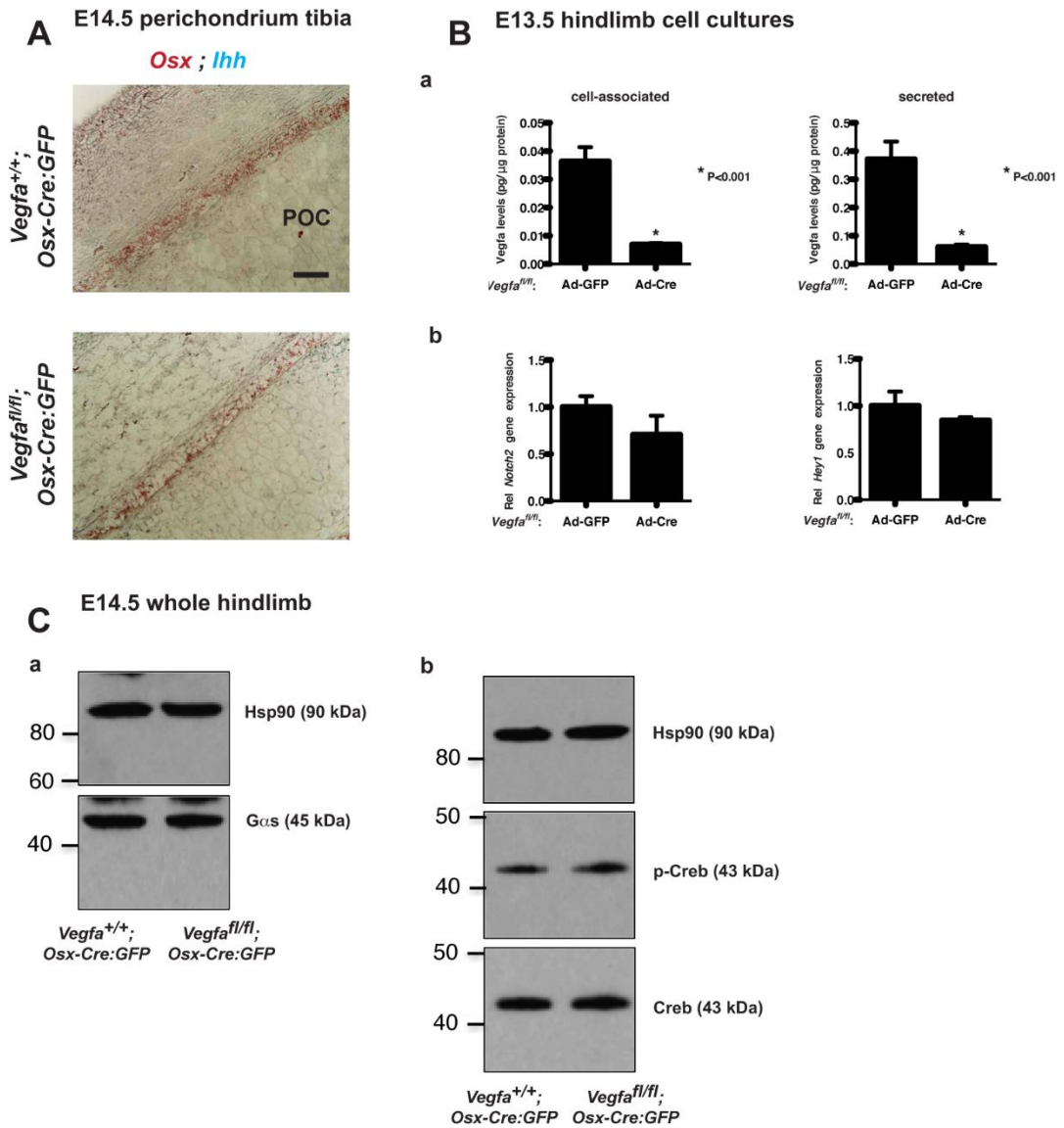


Fig. S4. Vegfa does not affect perichondrial Ihh expression and Gas and Pka-dependent pathways

(A) *In situ* hybridization on tibia sections (perichondrium area) from E14.5 *Vegfa^{+/+}; Osx-Cre:GFP* (top) and *Vegfa^{fl/fl}; Osx-Cre:GFP* (bottom) mice for *Osx* (red spots) and *Ihh* (turquoise spots) (scale bar: 50 μm). (B) (a) Vegfa protein levels measured by ELISA in cell-associated and secreted protein lysates of cultured hindlimb cells isolated from E13.5 *Vegfa^{fl/fl}* embryos treated with adenoviral Cre compared to adenoviral GFP (control). Vegfa protein levels normalized to total cellular proteins for each sample. Values represent mean Vegfa levels ± s.d. (n=3). (b) qRT-PCR of *Notch2* and *Hey1* expression in cultured hindlimb cells isolated from E13.5 *Vegfa^{fl/fl}* embryos, treated with adenoviral Cre, and induced to differentiate into the osteoblast lineage. Control cells were treated with adenoviral GFP. Relative gene expression levels normalized to levels of *Gapdh*. Values represent mean relative expression ± s.d. (n=3). (C) Western blotting of Gas (a) and phospho-Creb (Ser133) (b) in whole hindlimb lysates from E14.5 *Vegfa^{+/+}; Osx-Cre:GFP* (control) and *Vegfa^{fl/fl}; Osx-Cre:GFP* (mutant) mice; Hsp90 is loading control.

Supplementary Materials and Methods

Mouse Strains

Floxed *Vegfa*, *Flk1* and *Flt1* mice were crossed with Osx-Cre:GFP and described in our previous studies (Liu et al., 2012). Here we used additional crosses of mice carrying floxed alleles of *Vegfa*, *Flk1* and *Flt1* with *Col2-Cre*. Adult heterozygous 129-*Vegfamt1.1Nagy* mice were previously reported to have increased *Vegfa* protein levels as a consequence of the insertion of an IRES-NLS-lacZ-SV40pA sequence into the 3' UTR of the *Vegfa* gene locus resulting in removal of miRNA binding sites controlling inhibition of *Vegfa* mRNA translation (Cervi et al., 2007; Miquerol et al., 1999; Marneros, 2013). Analysis of whole hindlimb lysates from E14.5 129-*Vegfamt1.1Nagy* mice by Western blotting and ELISA assays showed that *Vegfa* protein levels were not significantly different from E14.5 WT controls (data not shown). For all timed pregnancies, male mice were mated with females overnight and separated in the morning, which was defined as E0.5. For harvesting of embryos, timed pregnant female mice were sacrificed by CO₂ exposure and the embryos were harvested after amnionectomy and removal of placenta. Genomic DNA isolated from portions of mouse tails were used for genotyping. All primers for genotyping are listed below.

Primer sequences used for genotyping

	forward primer	reverse primer	Product
Generic-Cre	5'-GATGAGGTTCGCAAGAACCTG-3'	5'-TGAACGAACCTGGTCGAAATC-3'	~ 350 bp
Vegfa	5'-CCTGGCCCTCAAGTACACCTT-3'	5'-TCCGTACGACGCATTCTAG-3'	~ 150 bp
Vegfr1	5'-CCTGCATGATTCTGATTGGA-3'	5'-GCCTAAGCTCACCTGCGG-3'	~ 180 bp
Vegfr2	5'-GACTTGTTCATCAGGCTAG-3'	5'-GACGCTGTTAAGCTGCTACAC-3'	~ 230 bp
Vegfa-LacZ	5'-ATCCTCTGCATGGTCAGGTC-3'	5'-CGTGGCCTGATTCAATTCC-3'	~ 300 bp
Vegfa-LacZ (positive control)	5'-CAAATGTTGCTTGTCTGGTG-3'	5'-GTCAGTCGAGTGACAGTTT-3'	~ 260 bp

Rosa Wildtype	5'-AAGGGAGCTGCAGTGGAGTA-3'	5'-CCGAAATCTGTGGGAAGTC-3'	~ 297 bp
Rosa Tomato Mutant	5'-CTGTTCCCTGTACGGCATGG-3'	5'-GGCATTAAAGCAGCGTATCC-3'	~ 169 bp

Skeletal Preparations and Staining

Skeletal structures of newborn mice (P1) were visualized by Alizarin Red (bone) and Alcian Blue (cartilage) staining. Skin, muscles and visceral organs were removed from mice prior to incubation in solution containing Alizarin Red S and Alcian Blue (Sigma-Aldrich). Skeletal samples were cleared by incubation in potassium hydroxide (1%) /glycerol (20%) solution and stored and photographed in glycerol.

Histology

Limbs of embryos and newborn mice were fixed in 4% paraformaldehyde (PFA) at 4°C overnight, infiltrated with 10%, 20% and 30% sucrose and embedded in OCT (Tissue-Tek®) compound (Sakura Finetek USA, Inc., Torrance, CA) for cryostat sectioning. 7.5 µm frozen sections were prepared for hematoxylin and eosin (H&E) staining, von Kossa staining, tartrate-resistant acid phosphatase (Trap) staining, bromodeoxyuridine (BrdU) staining, TUNEL staining and immunohistochemistry (IHC). For detection of mineralization, Von Kossa staining was performed by placing the frozen sections in 1% silver nitrate under a 60 Watt lamp for 90 minutes. The reaction was then stopped by putting sections in 2.5% sodium thiosulfate solution for 5 minutes and counterstained with 1% Safranin O solution. Trap staining for osteoclasts was performed using a Leukocyte Acid Phosphatase kit (Sigma-Aldrich) according to the manufacturer's instructions. Histological sections were taken with Nikon 80i Upright microscope using NIS-Elements AR3.1 software.

Immunohistochemistry (IHC) and immunocytochemistry (ICH)

IHC was performed according to Cell Signaling Technology protocols. Frozen sections of limbs were stained with CD31 (1:100; ab28364; Abcam), CD34 (1:100; ab81289; Abcam), Collagen I (1:100; ab21286; Abcam), Vegfr2 (1:50; sc-505; Santa Cruz Biotechnology), Vegfr1 (1:50; sc-316; Santa Cruz Biotechnology), β -catenin (1:500; C2206; Sigma-Aldrich) and Notch2 (1:1500; 5732; Cell Signaling) primary antibodies or normal rabbit IgG (sc-2027; Santa Cruz Biotechnology), and Alexa Fluor-conjugated secondary antibodies (1:200; Invitrogen). For ICH cells in culture chambers were fixed in 4% PFA and stained with Vegfa (1:50; sc-152; Santa Cruz Biotechnology) and Osx (1:50; sc-22538; Santa Cruz Biotechnology) primary antibodies, and Alexa Fluor-conjugated secondary antibodies (1:200; Invitrogen). All sections were mounted with HardSet Mounting Medium with DAPI (Vector Labs), observed and photographed using Nikon 80i Upright microscope or a Nikon Ti w/ Spinning Disk Confocal microscope. Control sections incubated with non-specific control IgGs did not show any staining. Images of the same optic fields were taken using blue, green and/or red fluorescence filters, and merged using MetaMorph Software.

X-Gal Staining

To detect Vegfa-lacZ reporter expression indicating *Vegfa* expression, E14.5 embryos or hindlimbs of newborn mice were fixed in 0.2% glutaraldehyde (EMS) and 2% PFA (BDH) for 30 minutes at room temperature, incubated in X-gal solution (1 mg/ml; Thermo Scientific) overnight at 30°C and post-fixed in 10% PFA overnight at room temperature. The bones were washed for 30 minutes in running water and then processed using a standard procedure for frozen sections.

RNA in situ hybridization

Frozen sections of limbs were processed for RNA in situ detection using the RNAscope 2-plex Detection Kit (Chromogenic) according to the manufacturer's instructions (Advanced Cell Diagnostics). RNAscope probes used include: Sp7 (NM_130458.3, region 837-2230), which was detected using the Fast Red detection reagent, and Col1a1 (NM_007742.3, region 1685-3051), Indian hedgehog (NM_010544.2, region 990-2336), Vegfa (NM_001025257.3, region 946-2156) and Col2a1 (NM_001113515.2, region 729-2036), which were detected using the Green detection reagent.

MicroCT

μ CT analyses were performed for hindlimbs of P9 mice using μ CT40 Scanco Medical, Zurich, Switzerland (10 mm isometric voxel resolution at 200 msec exposure, 2000 views and 5 frames per view).

Quantification of femur diameter, mineralization, Osx-Positive Cells, Trap staining, CD31 staining, CD34 staining, and Col1 staining

Diameter of P1 femurs was measured on four central-cut sections at least 30 μ m apart (n=3 animals per genotype). The total areas of mineralization, Trap staining and Osx/GFP-positive cells in P1 femurs were measured on the entire diaphysis of the femur, using ImageJ program. Three central-cut sections at least 22.5 μ m apart were analyzed per bone (n=3 animals per genotype). The invasion of endothelial cells and osteoclasts into the primary ossification center of E15.5 femurs were analyzed by comparing anti-CD31 staining and Trap staining in the primary ossification center of femur and total staining in a defined (Trap: 1100 x 1100 μ m; CD31: 1150 x 1150 μ m) region comprising the diaphysis of the femur. Three central-cut sections at least 22.5 μ m apart were analyzed per bone (n=3 embryos per genotype). Osx-positive cells in E14.5 and E15.5 tibia sections were counted in a defined (80 x 330 μ m) region comprising most of the

perichondrium, using ImageJ program. Three to six central-cut sections at least 22.5 μm apart were analyzed per bone (n=3 embryos per genotype). CD31 and CD34 stainings of E14.5 tibia sections were analyzed in a defined (190 x 1850 μm) region comprising most of the perichondrium, using ImageJ program. Three sections at least 22.5 μm apart were analyzed per bone (n=3 embryos per genotype). Col1 staining of E14.5 femur sections was analyzed in a defined (370 x 1480 μm) region comprising most of the perichondrium, using ImageJ program. Four to seven sections at least 30 μm apart were analyzed per bone (n=3 embryos per genotype).

Western Blotting

Protein lysates of hindlimbs of E14.5 embryos were prepared by adding ice-cold M-PER Mammalian Protein Extraction Reagent (Thermo Scientific) supplemented with cOmplete, Mini, EDTA-free protease inhibitor (Roche) and PhosSTOP phosphatase inhibitors (Roche). After centrifugation for 10 minutes (14,000 *rpm*) at 4°C, protein concentrations of supernatants were determined by Bradford Protein Assay kit (Thermo Scientific). Equal amounts of lysates were loaded and separated by SDS-polyacrylamide gel electrophoresis using 4-12% Bis-Tris precast polyacrylamide gels (NuPage; Invitrogen) followed by transfer of proteins onto nitrocellulose membranes (Bio-Rad). Protein was detected by probing the membranes overnight at 4°C using primary antibodies against phospho-Vegfr2 (1:1000; 2478; Cell Signaling), Vegfr2 (1:1000; 2479; Cell Signaling), Vegfr1 (1:500; sc-316; Santa Cruz Biotechnology), Ihh (1:1000; ab39634; Abcam), Gαs (1:500; sc-135914; Santa Cruz Biotechnology), phospho-Akt (1:1000; 9271; Cell Signaling), Akt (1:1000; 9272; Cell Signaling), phospho-Creb (1:1000; 9198; Cell Signaling), Creb (1:1000; 9197; Cell Signaling), β-catenin (1:1000; 9587; Cell Signaling), phospho-Gsk3β (1:1000; 9323; Cell Signaling), Gsk3β (1:1000; 9315; Cell Signaling), Notch2 (1:1000; 5732; Cell Signaling), phospho-p44/42 Mapk (1:1000; 9101; Cell Signaling), p44/42 Mapk (1:1000; 9102; Cell Signaling), Hsp90 (1:500; sc-13119; Santa Cruz Biotechnology), and β-actin

(1:5000; A5441; Sigma-Aldrich). Membranes were then incubated with horseradish peroxidase-conjugated secondary antibodies for 1 hour at room temperature and immunoreactive bands were detected by chemiluminescent substrate (Thermo Scientific).

BrdU incorporation and TUNEL staining

For BrdU incorporation, pregnant mice were injected i.p. with BrdU (Invitrogen) at 0.1 mg/g body weight two hours before sacrifice. E14.5 embryos were dissected and their limbs processed to obtain frozen sections. BrdU staining was performed using BrdU Staining Kit (Invitrogen) following manufacturer's instructions. For TUNEL staining, apoptotic cells were detected by using In Situ Cell Death Detection Kit, TMR Red (Roche) as described in manufacturer's instructions.

Mesenchymal Progenitor Cell Cultures

Hindlimbs of E13.5 embryos were dissected in Hanks Balanced Salt Solution (HBSS, Sigma-Aldrich) and digested in collagenase II (0.37 mg/ml), 0.25% dextrose in HBSS at 37°C for 90 minutes. Cells were disassociated by repetitive pipetting, centrifuged, resuspended in BGJb medium (Life Technologies) supplemented with 10% FBS, 1 x Antibiotics (Gibco), and plated in 12-well plates at 5×10^5 cells per well. Prior to reaching confluence cells were infected with either Ad-Cre or Ad-GFP overnight (Vector Biolabs). Cells were grown to confluence, induced to differentiate in the presence of β -glycerophosphate (8 mM; Sigma-Aldrich) and L-ascorbic acid phosphate (50 μ g/ml; Wako), and cultured for 5 days for Vegfa ELISA assays and 14 days for qRT-PCR. For rescue experiments cells were treated with recombinant mouse Vegfa (Vegf164) (50 ng/ml; 493-MV, R&D Systems) with or without Hedgehog antagonist GANT-58 (5 μ M; Sigma-Aldrich).

ELISA assays

Vegfa protein levels in cell lysates were assessed using the Quantikine Mouse VEGF Immunoassay (R&D Systems) in accordance with manufacturer's instructions; Vegfa protein levels assessed in cell lysates (cell-associated) or culture media (secreted) were normalized to total cellular proteins for each sample.

RNA extraction and gene expression analysis by qRT-PCR

Total RNA was extracted from cells using the RNeasy Isolation kit (Qiagen) according to the manufacturer's instructions. Then 1 µg of total RNA was used for cDNA synthesis using the RT² Easy First Strand kit (Qiagen) and PCR amplification of cDNA was performed using the iCycler iQ PCR system (Bio-Rad) using gene-specific primer sets listed below. Primers were designed using Primer3 software with parameters set for use with RT-PCR and PCR products were analyzed by gel electrophoresis to ensure the generation of a single product in the PCR reaction. Relative gene expression levels were normalized to the levels of the housekeeping gene *Gapdh*. All primers for qRT-PCR are listed below.

Primer sequences used for qRT-PCR

	forward primer	reverse primer
Gapdh	5'-GTGTTCCCTACCCCCAATGTG-3'	5'-AGGAGACAACCTGGCCTCA-3'
Runx2	5'-CCCAGCCACCTTACCTACA-3'	5'-TATGGAGTGCTGCTGGTCTG-3'
Sp7	5'-AGGCACAAAGAACGCCATACG-3'	5'-TGCAGGAGAGAGGAGTCCAT-3'
Col1a1	5'-TGACTGGAAGAGCGGAGAGT-3'	5'-GTTCGGGCTGATGTACCAAGT-3'
Ihh	5'-CCGAACCTTCATCTGGTGT-3'	5'-CCCCGAGAACATTGGAGTA-3'
Ptch1	5'-GAGACAAGCCCATCGACATT-3'	5'-CCAAGCGGTCAGGTAGATGT-3'
Gli1	5'-ACTAGGGGGCTACAGGAGGA-3'	5'-ACCTGGACCCCTAGCTTCAT-3'

Hhip	5'-TACTTGCCGAGGCCATATTTC-3'	5'-CTTCCCATCTGGCCCAAGTAG-3'
Notch2	5'-GATCGACAACCGACAGTGTG-3'	5'-GCGTTTCTTGGACTCTCCAG-3'
Hey1	5'-TGATGGACCGAGGTGTTGTA-3'	5'-TCCCTTCACCTCAC TGCTCT-3'

Supplementary References

- Cervi, D., Shaked, Y., Haeri, M., Usenko, T., Lee, C.R., Haigh, J.J., Nagy, A., Kerbel, R.S., Yefenof, E., and Ben-David, Y.** (2007). Enhanced natural-killer cell and erythropoietic activities in VEGF-A-overexpressing mice delay F-MuLV-induced erythroleukemia. *Blood* **109**, 2139-2146.
- Marneros, A.G.** (2013). NLRP3 inflammasome blockade inhibits VEGF-A-induced age-related macular degeneration. *Cell Rep.* **4**, 945-958.